Effects of glucose concentration and oxygen partial pressure on the respiratory metabolism of sheep temporomandibular joint disc cells

FANGRUI DONG[1], PENGFEI ZHANG[1], BIN MA[2], GUANGJIE BAO[2] and HONG KANG[1]

[1]Key Laboratory of Dental Maxillofacial Reconstruction and Biological Intelligence Manufacturing, School of Stomatology, Lanzhou University, Lanzhou, Gansu 730000; [2]Key Laboratory of Stomatology of State Ethnic Affairs Commission, Northwest Minzu University, Lanzhou, Gansu 730030, P.R. China

Received November 10, 2022; Accepted June 2, 2023

DOI: 10.3892/etm.2023.12086

Abstract. Temporomandibular joint (TMJ) disc degeneration is a common disease characterized by a decrease in metabolic function. The present study aimed to investigate the pathogenesis of TMJ disc degeneration by analyzing the effects of oxygen and glucose concentrations on metabolism in a simulated TMJ disc cell growth environment. Cell samples were divided into 10 groups and cultured in different nutritional environments, including 21 and 2% O_2 partial pressures and various glucose concentrations (0, 0.5, 3, 5.5 and 22.5 mmol/l). Cell proliferation, extracellular matrix content, mitochondrial function, and cell metabolism were subsequently analyzed. The results demonstrated that hypoxia and a low glucose concentration inhibited cell growth, and low glucose concentration inhibited extracellular matrix synthesis and adenosine 5'-monophosphate-activated protein kinase expression. Hypoxic conditions also induced a compensatory increase in the number of mitochondria, whereas mitochondrial deformation and swelling were observed in the absence of glucose. According to this study, the primary metabolic pathway of TMJ disc cells is glycolysis. It was concluded that hypoxic conditions and normal glucose concentrations are needed for the growth of TMJ disc cells. Glucose is necessary to ensure cell survival, extracellular matrix synthesis and mitochondrial function. Glucose deficiency may be related to disc degeneration, aging and disease mechanisms.

Correspondence to: Professor Hong Kang, Key Laboratory of Dental Maxillofacial Reconstruction and Biological Intelligence Manufacturing, School of Stomatology, Lanzhou University, 199 Dong Gang Xi Road, Lanzhou, Gansu 730000, P.R. China
E-mail: kanghong@lzu.edu.cn

Professor Guangjie Bao, Key Laboratory of Stomatology of State Ethnic Affairs Commission, Northwest Minzu University, 1 Xibei Xincun Road, Lanzhou, Gansu 730030, P.R. China
E-mail: 2645784430@qq.com

Key words: oxygen partial pressure, glucose concentration, temporomandibular joint disc, degeneration, extracellular acidification rate, oxygen consumption rate

Introduction

Temporomandibular joint disorder (TMD) is a common disease, which affects up to 15% of adults (1). Degeneration of the temporomandibular joint (TMJ) disc is the most common concomitant symptom of temporomandibular disorders (TMDs) (2), which compromises the therapeutic efficacy of TMD treatment (3). At present, the most commonly used methods to treat TMD in the clinic include occlusal splint therapy, drugs, intra-articular injection, discectomy and joint replacement. However, the efficacy of various treatment methods cannot be guaranteed. Because these traditional treatment methods cannot reverse the dysfunctional TMJ tissue, TMD cannot be fully cured and the patients' pain may not be completely relieved (4). The causative factors in disc degeneration are unclear (5), although studies have suggested that aging (6), inflammation (7) and biomechanical factors (8) are implicated. One hypothesis is that insufficient nutrient supply and energy metabolism disorders in TMJ discs may lead to disc degeneration, although evidence for this is lacking (9-11).

Glucose and oxygen are necessary to maintain cellular nutrition and metabolic homeostasis (12,13), both of which are vital for articular disc development and extracellular matrix synthesis (14). Glucose and oxygen levels are typically lower in non-vascular connective tissues, such as articular cartilage and discs, than in blood and tissue fluids (15). Intervertebral disc cells and chondrocytes are typically classified as high glycolytic cells (16,17). By contrast, TMJ disc cells have a higher cell density and higher oxygen consumption than intervertebral discs and articular cartilage (18), and are more susceptible to disease caused by impaired nutrient supply (19,20). Our prior study of the effects of different oxygen partial pressures on the growth and proliferation of sheep TMJ disc cells found that hypoxic conditions (2% O_2) favored cell survival (21,22). However, it is unlikely that the TMJ discs are affected solely by hypoxia or glucose alone (23). Given the steep nutrient gradient in the TMJ disc, we designed experimental groups with glucose at concentrations of 0, 0.5, 3 and 5.5 mmol/l and

a control group with high sugar medium (25 mmol/l). Oxygen partial pressure was designed to be at normal (21% O_2) and hypoxic (2% O_2) levels. This allowed the investigation of cell proliferation, synthesis and energy metabolism. The respiratory metabolism pathways in TMJ disc cells and the effects of oxygen and glucose concentrations were elucidated to study the pathogenesis of TMJ disc degeneration.

Materials and methods

Experimental groups. A total of 10 experimental groups were constructed. Five were normoxic (21% O_2), with glucose concentrations of 0 (NG1), 0.5 (NG2), 3 (NG3), 5.5 (NG4) and 22.5 mmol/l [negative control (NC)]. The remaining groups were hypoxic (2% O_2) and exposed to the same glucose concentrations: 0 (HG1), 0.5 (HG2), 3 (HG3), 5.5 (HG4) and 22.5 mmol/l [hypoxic control (HC)].

Cell isolation and culture. TMJ disc cells were isolated and extracted from 12 discs of six fresh heads of 3-6-month-old healthy sheep, which were purchased from slaughterhouses, as described previously (22). Sheep heads were cleaned and soaked in 75% alcohol for 30 min. Bilateral temporomandibular discs were removed in whole pieces under aseptic conditions, and the ligaments around the disc and the attached muscles were removed. The cells were digested with 0.2% collagenase type I (cat. no. SCR103; Sigma-Aldrich) for ~15 h at 37˚C in a water bath shaker at 80 x g and collected by centrifugation. Primary cells were cultured in DMEM (cat. no. 10313-021; Gibco; Thermo Fisher Scientific, Inc.), 10% FBS [cat. no. 04-001-1A; Biological Industries (BI)] and 1% penicillin-streptomycin solution (cat. no. 03-031-1B; BI). The cells were incubated at 37˚C in a 5% CO_2 incubator. All animal procedures were approved by The Animal Ethics Committee of the School of Stomatology, Northwest Minzu University (Lanzhou, China) and complied with its requirements (approval no. XBMZ YX-2021004).

Cell proliferation. Third generation (p3) sheep TMJ disc cells were seeded in 96-well plates at a density of 6,000 cells/well and tested after 1, 2, 3, 6 and 9 days of incubation at 37˚C under different glucose and oxygen conditions. The Cell Counting Kit-8 (CCK-8) assay (cat. no. CA1210-100T; Beijing Solarbio Science & Technology) was performed by uniformly replacing the complete culture media with 200 μl fresh media containing 10 μl CCK-8 solution, gently shaking the plate to mix the liquid, and incubating for 4 h. The absorbance was measured at 450 nm using a microplate reader. The results reflected cell proliferation.

Reverse transcription-quantitative PCR (RT-qPCR). RNA was extracted from p3 sheep TMJ disc cells cultured in 6-well plates at a density of $1x10^5$ cells/well for 9 days under the above-mentioned different nutritional conditions. RNA extraction was performed using a Quick-RNA Viral Kit (cat. no. D3015; Zymo Research Corp). Then, RNA was reverse transcribed using a HiScript II 1st Strand cDNA Synthesis Kit (cat. no. R211-01; Vazyme Biotech Co., Ltd.). The reaction was conducted at 50˚C for 15 min and 85˚C for 5 sec to obtain cDNA products, and the mixture was then stored at 4˚C. The qPCR system was configured according to the instructions of the ChamQ SYBR qPCR Master Mix (High ROX Premixed; cat. no. Q341-02; Vazyme Biotech Co., Ltd.). The standard procedure for the PCR amplification was as follows: Pre-denaturation at 95˚C for 10 min, for 1 cycle; thermal cycling at 95˚C for 15 sec, 60˚C for 15 sec, and 72˚C for 30 sec, for 40 cycles. The primer sequences used are provided in Table I. GAPDH was selected as the internal reference gene. The $F=2^{-\Delta\Delta Cq}$ method was used to quantify data and calculate the relative expression level of the target gene (24). The expression of the NC group was set to F=1 and all other experimental groups were compared with it.

Flow cytometric analysis. The p3 sheep TMJ disc cells were cultured in 6-well plates at a density of $1x10^5$ cells/well for 9 days at 37˚C with the same 10 groups as above. The cells were digested and centrifuged three times and the supernatant was discarded. The mitochondria were stained using Mito-tracker Green (cat. no. C1048; Bi Yun Tian Biologicals) and the staining solution was diluted according to the manufacturer's instructions. Subsequently, 1 ml of pre-warmed (37˚C) Mito-Tracker Green was added to the samples and then incubated for 15-30 min. Following this, cells were resuspended in PBS. Samples were detected using an image flow cytometer (model Amnis® FlowSight; Luminex Corporation) and the results were analyzed using IDEAS 1.0 software provided by the above company.

Mitochondrial morphology. The p3 sheep TMJ disc cells were cultured in Petri dishes at a density of $1x10^5$ cells/well for 9 days at 37˚C with the same 10 groups as above. Then, 1 ml of diluted Mito-tracker Green (the dye solution at a ratio of 1:10,000) was added to each culture dish and incubated for 15-30 min. The staining solution was aspirated and 1 ml Hoechst 33258 (cat. no. C1011; Bi Yun Tian Biologicals) was added to the cells for 10 min to stain the nuclei. The samples were observed and imaged by confocal laser scanning microscopy (CLSM; model Olympus FV3000; Olympus Corporation). Image processing and acquisition were finished via Olympus TruSight provided by Olympus Corporation.

Glycolysis stress test. The p3 sheep TMJ disc cells were seeded at $1x10^4$ cells/well in XFe 24-well cell culture plates. The test was performed after 3 and 9 days of incubation at 37˚C with the same 10 groups as above. On the day of the assay, the plates were washed three times with the Seahorse XF media (without serum, glucose, or bicarbonate, but with the addition of 2 mM glutamine. cat. no. 103575-100; Agilent Technologies, Inc.). Then, the Seahorse XF Glycolysis Stress Test Kit (cat. no. 103020-100; Agilent Technologies, Inc.) reagents were added according to the manufacturer's instructions. The Seahorse XFe24 analyzer (Agilent Technologies, Inc.) was used to measure glycolysis stress.

Enzyme-linked immunosorbent assay (ELISA). The p3 sheep TMJ disc cells were cultured in 6-well plates at a density of $1x10^5$ cells/well for 1, 2, 3, 6, 9 days at 37˚C with the same 10 groups as above. The cells were resuspended using PBS and the cell concentration was adjusted to ~10^6 cells/ml. The samples were rapidly frozen and thawed five times to release the cell contents

Table I. Primers used in reverse transcription-quantitative PCR.

Gene	Primer sequences (5'-3')	bp
GAPDH	F: CAAGTTCCACGGCACAGTCA	20
	R: GGTTCACGCCCATCACAAA	19
Col-I	F: CCTGCGTACAGAACGGCCT	19
	R: ACAGCACGTTGCCGTTGTC	19
Col-II	F: AGCAGCAAGAGCAAGGACAAG	21
	R: TTCTTGCAGTGGTAGGTGATGTT	23
Aggrecan	F: GTCCACCATTCGGCATAACC	20
	R: TGGGGTCACTTCAACCAAACT	21
GLUT1	F: CTGGTTCTGTTCTTCATCTTCACCT	25
	R: TTGTCACTTTGGCTTGCTCCT	21
AMPKα1	F: GACTGCTACTCCACAGAGATCG	22
	R: TCAGCATCTGAATCACTCCTTT	22

F, forward; R, reverse; Col-I, collagen type I; GLUT1, glucose transporter 1; AMPKα1, adenosine 5'-monophosphate-activated protein kinase subunit α1.

and the supernatant was collected. The concentrations of lactate dehydrogenase (LDH), reactive oxygen species (ROS) and superoxide dismutase (SOD) were measured using the Sheep Lactate Dehydrogenase (LDH) ELISA Kit (cat. no. SP18658; WuHan Saipei Biotechnology Co, Ltd), Sheep Reactive Oxygen Species (ROS) ELISA Kit (cat. no. SP19258; WuHan Saipei Biotechnology Co, Ltd.) and Sheep Superoxide Dismutase (SOD) ELISA Kit (cat. no. SP18814; WuHan Saipei Biotechnology Co, Ltd.). The samples were processed according to the manufacturer's instructions and analyzed using a microplate reader with a wavelength of 450 nm. The experimental results were calculated by drawing a standard curve following the manufacturer's instructions.

Statistical analysis. All data were presented as the mean ± SD and all experiments were repeated at least three times with similar results. GraphPad Prism 8.0 software (GraphPad Software; Dotmatics) was used to perform all statistical analyses, and two-way ANOVA followed by Tukey's test was used to compare the differences between groups. $P<0.05$ was considered to indicate a statistically significant difference.

Results

Hypoxia and low glucose inhibit cell growth. Cell proliferation assays demonstrated that under normoxic conditions, TMJ disc cell culture densities reached an OD_{450} of 2.0 on day 6. Different glucose concentrations had no significant effect on proliferation over 9 days ($P=0.567$; Fig. 1A). Under hypoxic conditions, there was no significant difference for the first 3 days ($P=0.875$), but on day 6, cell proliferation decreased significantly in the HG1 (0.367±0.092) and HG2 (0.46±0.124) groups, as proliferation stopped and apoptosis was initiated with the OD_{450} remaining <1.0 (Fig. 1B), which may indicate the cessation of cell proliferation and the onset of apoptosis. The remaining groups (HG3, HG4 and HC) showed continued but slowed proliferation compared with HG1 and HG2. On day 9, the OD_{450} values reached 2.0 for HG3 (2.137±0.129), HG4 (2.118±0.177) and HC (2.073±0.252) groups (Fig. 1B), which suggested that glucose concentrations ≥3 mmol/l resulted in an increase in TMJ cell proliferation.

Low glucose concentration affects extracellular matrix synthesis and adenosine 5'-monophosphate-activated protein kinase subunit α1 (AMPKα1) expression. The main components of the extracellular matrix of TMJ disc cells are collagen type I (Col-I), Col-II and aggrecan, the expression levels of which were measured using RT-qPCR (Fig. 2A-C). Col-I expression under normoxic conditions in each group was as follows: compared with NC (1.00±0.106), NG1 (0.542±0.086; $P<0.0001$) and NG2 (0.854±0.021; $P=0.0033$), were significantly reduced, versus the significant increase in NG3 (1.508±0.037; $P<0.0001$) and NG4 (1.610±0.057; $P<0.0001$) (Fig. 2A). Expression under hypoxic conditions was lower in HG1 (0.091±0.006; $P<0.0001$) and HG2 (0.189±0.010; $P<0.0001$) than in the HC (0.415±0.082) group (Fig. 2A). There was no difference in the HG3 group (0.482±0.023; $P=0.4082$, $P>0.05$), however, Col-I in the HG4 group (0.655±0.014; $P=0.0002$) significantly increased compared with HC. Regardless of oxygen concentration, the expression of Col-I was highest in the 5.5 mmol/l glucose (NG4 and HG4 groups), but was significantly lower in hypoxic conditions than in normoxic conditions ($P<0.0001$).

The level of Col-II expression, as shown in Fig. 2B, increased with increasing glucose concentration. Under normoxic conditions, NG1 (0.209±0.071; $P<0.0001$), NG2 (0.706±0.136; $P=0.0019$), NG3 (0.887±0.074; $P>0.05$) and NG4 (0.946±0.092; $P>0.05$) exhibited lower levels of Col-II expression than the NC group (1.00±0.086), but there was no statistical significance between NG3 and NG4. Under hypoxic conditions, Col-II expression in HG1 (0.134±0.040; $P<0.0001$), HG2 (0.564±0.079; $P<0.0001$) and HG3 (0.836±0.077; $P=0.0034$) was significantly lower than that in the HC group (1.122±0.124), and there was no significant difference in the HG4 group (0.940±0.085; $P>0.05$). There was also no significant difference in Col-II expression between the hypoxic and normoxic conditions ($P>0.05$).

Aggrecan expression was significantly upregulated in the NC group ($P<0.0001$; Fig. 2C), but was low under all other test conditions. In general, the aggrecan expression levels in the normoxia groups were higher than those in the hypoxia groups.

Glucose transporter 1 (GLUT1) is the primary glucose transporter in chondrocytes (24). GLUT1 expression increased in high glucose concentrations (Fig. 2D). Under normoxic conditions, GLUT1 expression was significantly lower in NG1 (0.086±0.003; $P<0.0001$), NG2 (0.160±0.023; $P<0.0001$), NG3 (0.710±0.035; $P<0.0001$), and NG4 (0.861±0.060; $P=0.0080$) groups when compared with the NC group (1.00±0.090). Under hypoxic conditions, the HG1 (0.173±0.049; $P<0.0001$), HG2 (0.311±0.039; $P<0.0001$), and HG3 (0.724±0.009; $P=0.0052$) groups had lower GLUT1 concentrations than the HC group (0.871±0.058). HG4 (0.901±0.053; $P>0.05$) was slightly higher than the HC group, but this difference was not statistically significant. GLUT1 expression was essentially unaffected by oxygen partial pressure.

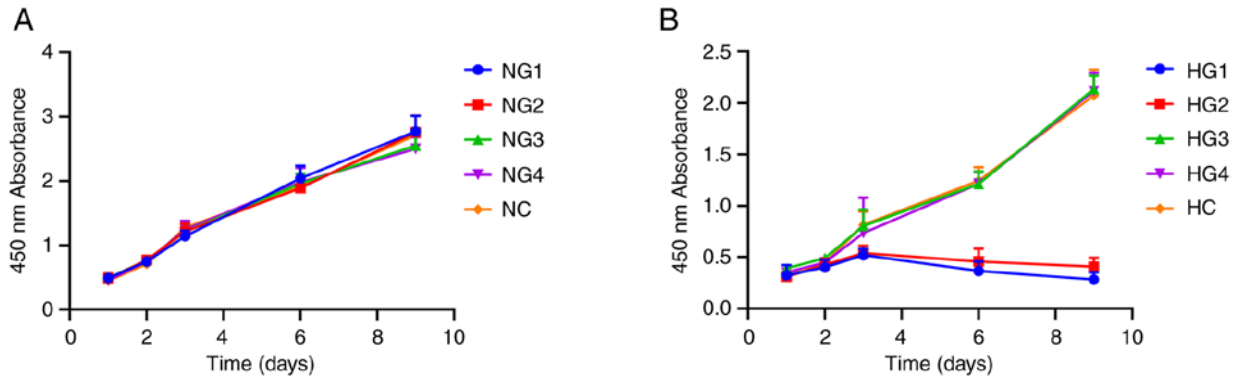

Figure 1. Effects of different glucose concentrations on the proliferation of sheep temporomandibular joint disc cells. (A) Cell proliferation curve of cells in normoxic conditions. (B) Cell proliferation curve of cells in hypoxic conditions. NG1, normoxia and 0 mmol/l glucose group; NG2, normoxia and 0.5 mmol/l glucose group; NG3, normoxia and 3 mmol/l glucose group; NG4, normoxia and 5.5 mmol/l glucose group; NC, normoxia and control group (22.5 mmol/l); HG1, hypoxia and 0 mmol/l glucose group; HG2, hypoxia and 0.5 mmol/l glucose group; HG3, hypoxia and 3 mmol/l glucose group; HG4, hypoxia and 5.5 mmol/l glucose group; HC, hypoxia and control group (22.5 mmol/l).

AMPK is a key molecule in the regulation of biological metabolism (25). Under normoxic conditions, AMPKα1 expression increased at high glucose concentrations (Fig. 2E). NG1 (0.233±0.003; P<0.0001), NG2 (0.293±0.005; P<0.0001), NG3 (0.496±0.007; P<0.0001), and NG4 (0.897±0.050; P=0.0046) groups exhibited significantly downregulated AMPKα1 expression, compared with the NC group (1.00±0.080). The trends were similar under hypoxic conditions. The trend of AMPKa1 expression in both normoxia and hypoxia was up-regulated with increasing sugar concentration, indicating that sufficient glucose could activate the expression of AMPKa1.

Hypoxia causes a compensatory increase in the number of mitochondria. MitoTracker Green mitochondrial staining and flow cytometry were used to observe the number of mitochondrial in TMJ disc cells under normoxic and hypoxic conditions (Fig. 3A-G). In Fig. 3A-E, CH01 panels show images under light microscopy observation, and the CH02 panels show fluorescence images observed after mitochondrial staining. Fluorescence intensity values reflect the relative number of mitochondria. Compared with the normoxic samples, fluorescence was significantly higher in the hypoxic samples (P<0.0001) and increased with increasing glucose concentrations. All groups were significantly different from the control group (P<0.0001; Fig. 3G).

Mitochondrial deformation and swelling in the absence of glucose. In the G1 group, under both normoxic and hypoxic conditions (NG1 and HG1, respectively), the mitochondrial morphology was swollen and shorter and the mitochondrial network was absent (Fig. 4A and C) compared with the controls (Fig. 4B and D), in which the mitochondria were evenly distributed in the cytoplasm surrounding the nucleus and connected in a network. Compared with the normoxic control group (NC), the mitochondrial morphology in the hypoxic control group (HC) was slightly shorter and the network was less clear.

Glycolysis is the primary metabolic pathway of TMJ disc cells. The glycolytic pathway is significantly enhanced when cells are well nourished. When nutrition is insufficient, metabolic pathways are inhibited. The Seahorse XFe glycolysis stress test was used to detect the extracellular acidification rate (ECAR) and oxygen consumption rate (OCAR). This experiment detected glycolysis after the addition of glucose and 2-deoxy-D-glucose. The values express the basic glycolytic ability and potential of cells. Glycolysis ability represents the level of glycolysis of cells under normal nutrient supply. Glycolysis potential represents the maximum glycolysis level of cells when the oxidative phosphorylation pathway is inhibited.

There was no significant difference in the basic glycolysis rate after 3 days under normoxic conditions. Cultures exposed to lower glucose concentrations had a greater glycolysis potential and stronger glycolysis ability (Fig. 5A). After 9 days in a normoxic environment, the glycolytic ability and potential of cells in the low glucose group had improved (P<0.0001; Fig. 5B).

After three days in a hypoxic environment, the basic glycolysis rate of TMJ disc cells increased with increasing glucose concentrations (Fig. 5C). On day nine, the basic glycolysis rate and ability of glycolysis of the cells decreased significantly (Fig. 5D). The overall detection of glycolysis was lower in hypoxia than in normoxia (P<0.0001).

The Seahorse XFe glycolysis stress test also showed the basic OCAR. In normoxia, the OCAR decreased with increasing glucose concentrations (Fig. 5E). In hypoxia, the OCAR was the highest in the HG4 group and increased with increasing glucose concentration but remained significantly lower than in normoxic conditions (P<0.0001; Fig. 5F).

Some respiratory metabolites remain at normal levels in the short term. LDH, ROS, and SOD levels were detected using an ELISA kit, as LDH is the key enzyme in glycolysis, ROS is a product of oxidative phosphorylation, and SOD is an antagonist of ROS and is used as a detection index.

The content of LDH under normoxic conditions decreased gradually over time (P<0.0001; Fig. 6A). However, differences in glucose concentration yielded no significant differences in LDH, ROS or SOD concentrations (P>0.05; Fig. 6A-C). Under hypoxic conditions, LDH concentration gradually increased with increasing glucose concentrations (Fig. 6D). On day 9,

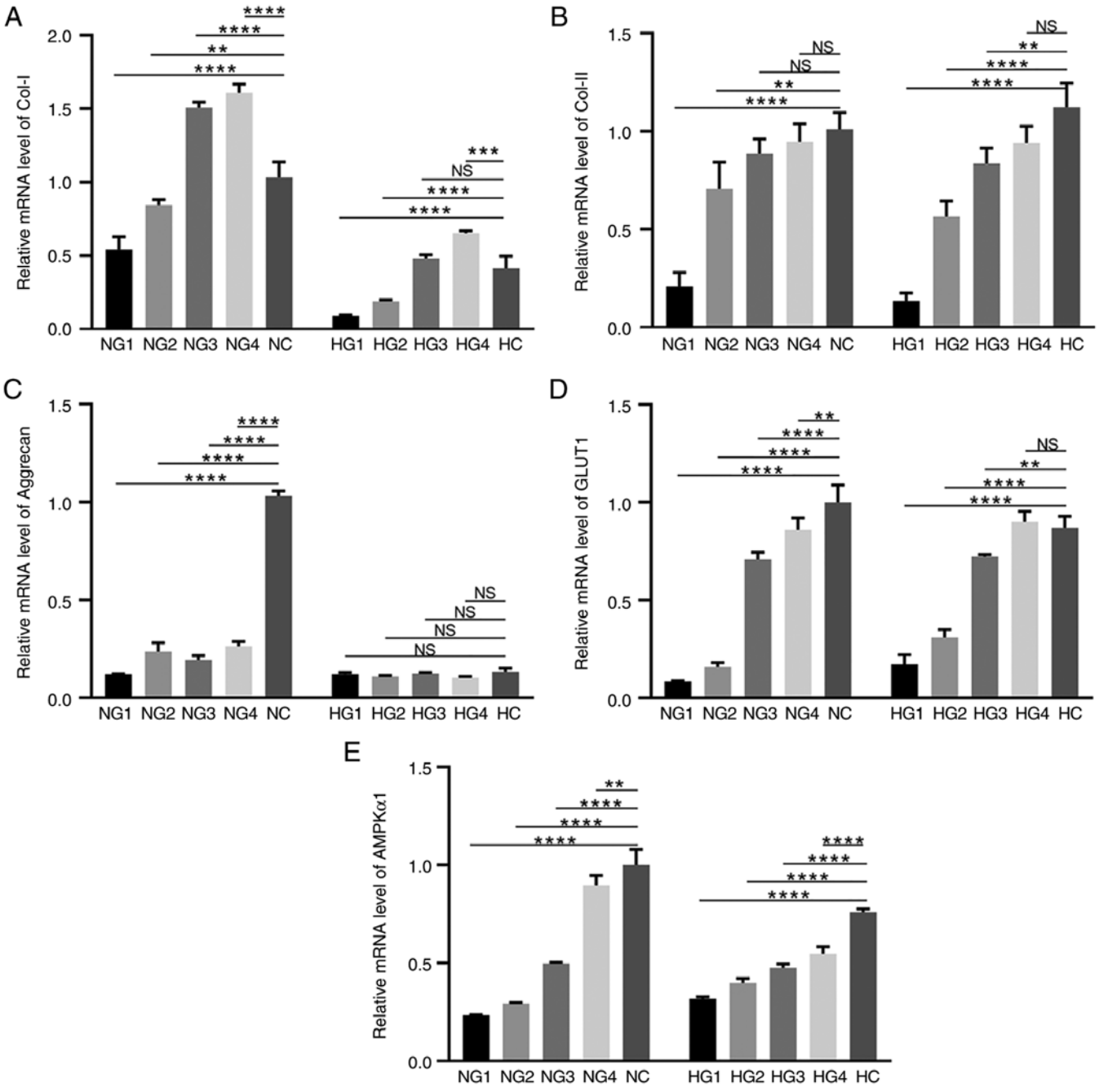

Figure 2. Expression levels of extracellular matrix and cell metabolism-related molecules. (A) The mRNA expression level of Col-I. (B) The mRNA expression level of Col-II. (C) The mRNA expression level of aggrecan. (D) The mRNA expression level of GLUT-1. (E) The mRNA expression level of AMPKα1. **P<0.01, ***P<0.001, ****P<0.0001. NS, not significant; Col-I, collagen type I; GLUT-1, glucose transporter 1; AMPKα1, adenosine 5'-monophosphate-activated protein kinase subunit α1; NG1, normoxia and 0 mmol/l glucose group; NG2, normoxia and 0.5 mmol/l glucose group; NG3, normoxia and 3 mmol/l glucose group; NG4, normoxia and 5.5 mmol/l glucose group; NC, normoxia and control group (22.5 mmol/l); HG1, hypoxia and 0 mmol/l glucose group; HG2, hypoxia and 0.5 mmol/l glucose group; HG3, hypoxia and 3 mmol/l glucose group; HG4, hypoxia and 5.5 mmol/l glucose group; HC, hypoxia and control (22.5 mmol/l) group.

compared with the HC group (31.226±0564 U/ml), the LDH content was significantly lower in the HG1 (10.723±0.779 U/ml; P<0.0001) and HG2 (982.826±25.171 U/ml; P<0.0001) groups. In the HG3 (34.789±0.508 U/ml; P=0.000191) and HG4 (35.435±0.529 U/ml; P=0.000045) groups, the LDH concentration was slightly higher than that in the HC group.

Under hypoxic conditions, there was no significant difference in ROS concentration between the different glucose groups within the first 3 days (P=0.348; Fig. 6E). On day 9, the ROS concentration in the HG1 (825.123±26.915 U/ml; P=0.000072) and HG2 (982.826±25.171 U/ml; P=0.005) groups were significantly lower than that in the HC group (1,202.200±49.208 U/ml) (Fig. 6E). However, the ROS concentration in the HG3 (1,146.631±68.128 U/ml, P=0.747) and HG4 (1,153.435±86.183 U/ml; P=0.882) groups was not significantly different from that in the HC group.

The SOD concentration in cells in normoxic conditions increased over time, with no significant difference between

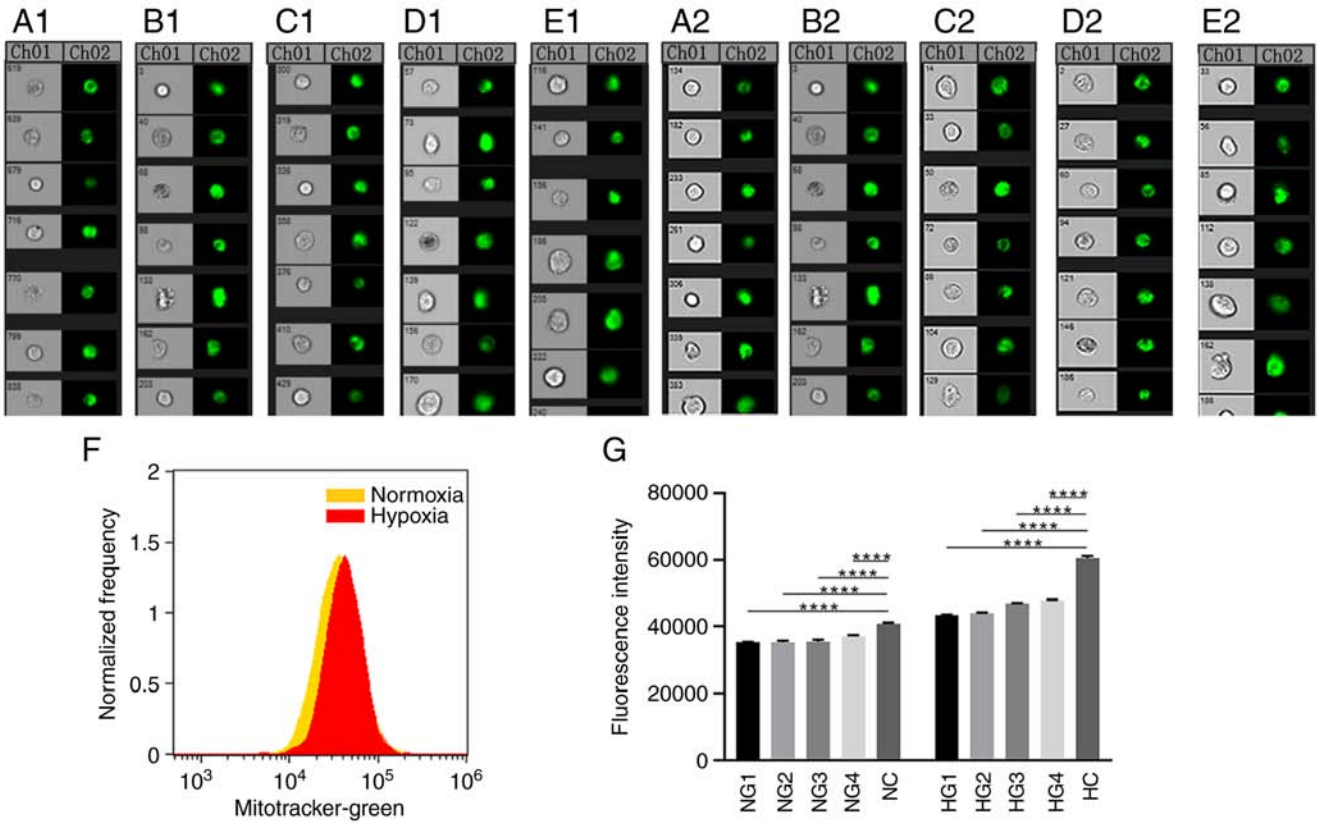

Figure 3. Flow cytometry results of Mito-tracker Green mitochondrial probe staining. (A1) Flow cytometry cell images of normoxia and 0 mmol/l glucose group; (B1) flow cytometry cell images of normoxia and 0.5 mmol/l glucose group; (C1) flow cytometry cell images of normoxia and 3 mmol/l glucose group; (D1) flow cytometry cell images of normoxia and 5.5 mmol/l glucose group; (E1) normoxia and control (22.5 mmol/l) group; (A2) flow cytometry cell images of hypoxia and 0 mmol/l glucose group; (B2) flow cytometry cell images of hypoxia and 0.5 mmol/l glucose group; (C2) flow cytometry cell images of hypoxia and 3 mmol/l glucose group; (D2) flow cytometry cell images of hypoxia and 5.5 mmol/l glucose group; (E2) flow cytometry cell images of hypoxia and control (22.5 mmol/l) group; (F) mito-tracker green mitochondrial probe staining fluorescence intensity diagram. (G) Fluorescence intensity analysis of mito-tracker green mitochondrial probe staining. ****P<0.0001, NS, not significant.

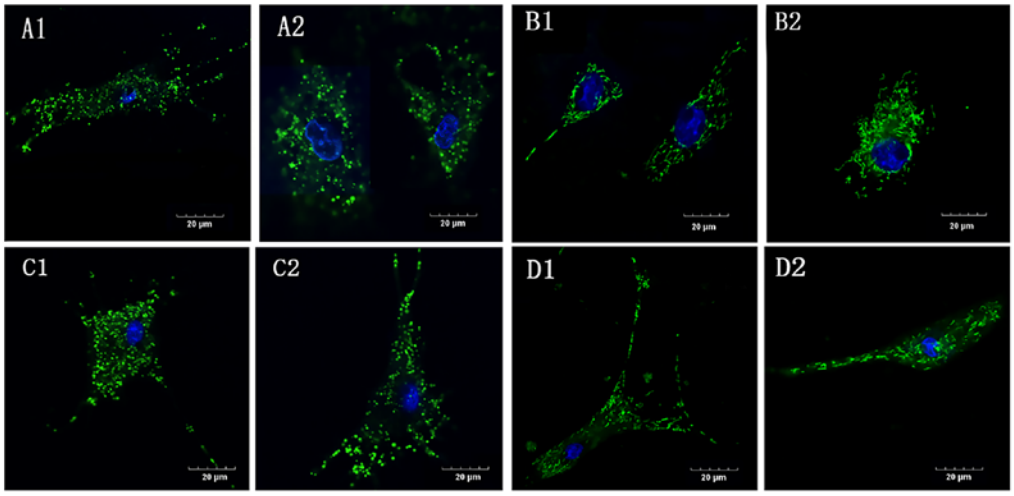

Figure 4. CLSM images of mitochondrial staining in sheep TMJ disc cells (magnification x60; scale bar, 20 μm). (A1-A2) CLSM images of normoxia and 0 mmol/l glucose group; (B1-B2) CLSM images of normoxia and control (22.5 mmol/l) group; (C1-C2) CLSM images of hypoxia and 0 mmol/l glucose group; (D1-D2) CLSM images of hypoxia and the control (22.5 mmol/l) group. The green staining shows mitochondria and the blue staining shows the nucleus of the TMJ disc cells. CLSM, confocal laser scanning microscopy; TMJ, temporomandibular joint.

groups (P=0.440; Fig. 6C). The SOD concentration in cells under hypoxic conditions also increased over time (Fig. 6F) but remained only slightly higher than that under normoxic conditions (the first 6 days, P<0.0001; on day 9, P=0.0183). On day 9, SOD levels in HG1 (438.808±17.860 U/ml; P=0.000002) and HG2 (413.990±10.483 U/ml; P=0.000026) were significantly higher than those in HC (339.338±3.691 U/ml); furthermore, SOD levels in HG3 (352.630±6.134 U/ml; P=0.506) and HG4

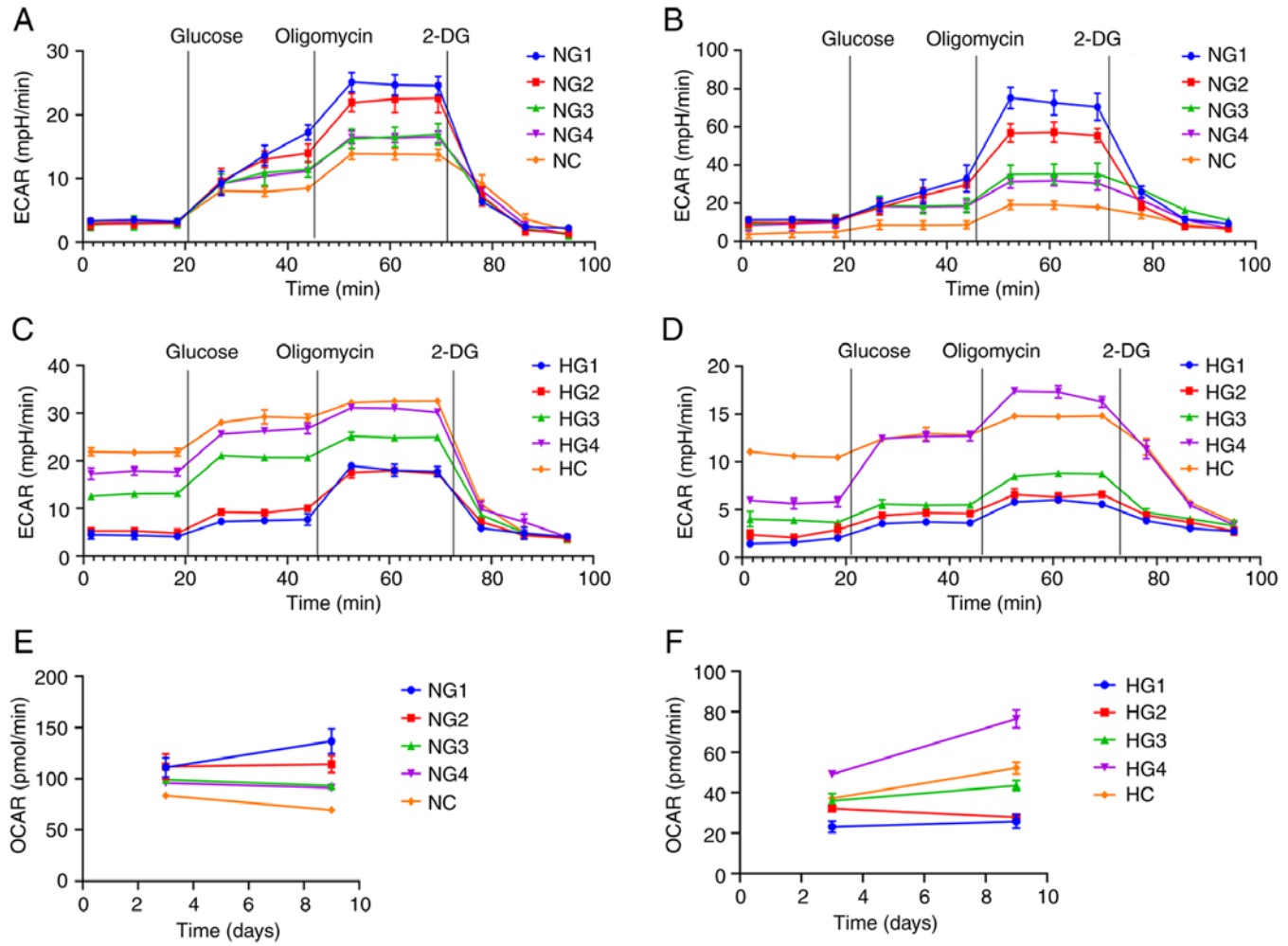

Figure 5. Glycolysis pressure test results. (A) ECAR after 3 days under normoxic conditions. (B) ECAR after 9 days under normoxic conditions. (C) ECAR after 3 days under hypoxic conditions. (D) ECAR after 9 days under hypoxic conditions. (E) OCAR after 3 and 9 days under normoxic conditions. (F) OCAR after 3 and 9 days under hypoxic conditions. ECAR, extracellular acidification rate; OCAR, oxygen consumption rate; NG1, normoxia and 0 mmol/l glucose group; NG2, normoxia and 0.5 mmol/l glucose group; NG3, normoxia and 3 mmol/l glucose group; NG4, normoxia and 5.5 mmol/l glucose group; NC, normoxia and control (22.5 mmol/l) group; HG1, hypoxia and 0 mmol/l glucose group; HG2, hypoxia and 0.5 mmol/l glucose group; HG3, hypoxia and 3 mmol/l glucose group; HG4, hypoxia and 5.5 mmol/l glucose group; HC, hypoxia and control (22.5 mmol/l) group.

(362.225±3.427 U/ml; P=0.102) were higher but the differences were not significant (Fig. 6F).

Discussion

A study has shown that glucose is a key nutrient for maintaining cell survival in non-vascular tissue (26). For example, bovine nucleus pulposus cell viability decreases significantly in the absence of glucose, regardless of oxygen concentration (27). In addition, a study investigating the energy metabolism of porcine TMJ disc cells showed that glucose was a limiting nutrient for survival. Hypoxia also limits the production of intracellular ATP and the synthesis of extracellular collagen and proteoglycan (23). This is consistent with the results of the present study. The present study demonstrated that in hypoxic conditions, the number of cellular mitochondria increased, Col-II and aggrecan expression did not change significantly, and cellular glucose uptake and AMPKα1 levels were also unaffected. This suggested that hypoxia does not cause cellular damage or lead to degeneration in TMJ disc cells. By contrast, low-glucose conditions yielded changes in mitochondrial morphology (causing the organelle to appear degenerated and swollen) and significantly inhibited the expression of extracellular matrix synthesis-associated Col-I, Col-II and aggrecan and the expression of GLUT and AMPKα1, all of which may contribute to degeneration in TMJ disc cells.

Mitochondria are critical in cell aging and age-related diseases (28). The loss of mitochondrial function leads to the shortening of cell telomeres, which in turn leads to aging (29). Mitochondria are essential for maintaining equilibrium between redox reactions and energy metabolism in cells and are critical for cell survival and death (30). The expression of AMPK has a significant impact on mitochondrial function and is therefore a key factor in cellular degeneration and aging (31). AMPK is located in the mitochondria and can be activated in the absence of glucose; it stimulates the regeneration of new mitochondria, promotes the autophagy of aging mitochondria and maintains the dynamic balance of mitochondrial numbers (25). Furthermore, decreased levels of mitochondrial function and AMPK activity have also been observed in degenerative cartilage, aging cartilage, and biomechanically injured bovine cartilage (32,33). This decrease in

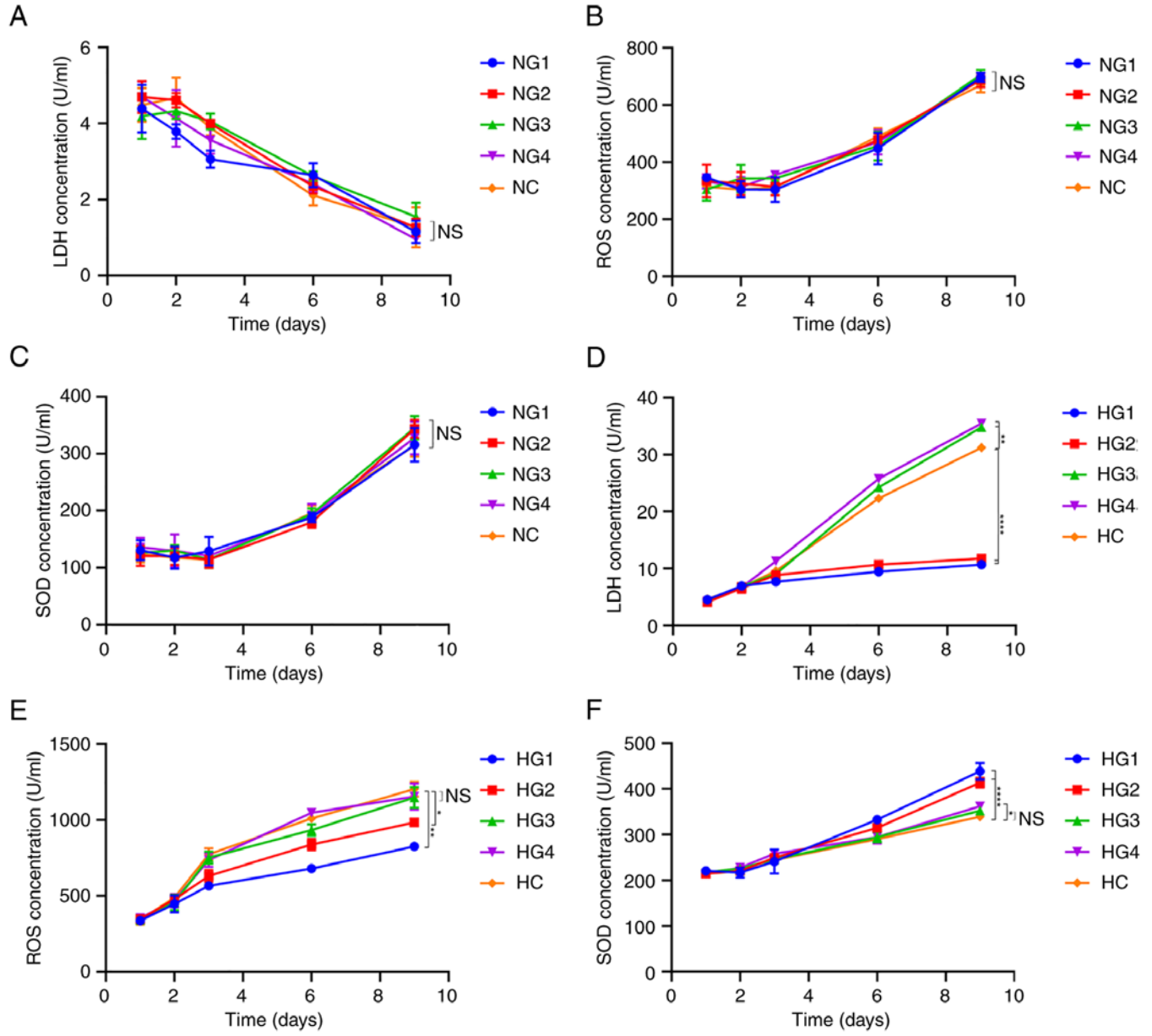

Figure 6. Concentration of respiratory metabolism-related molecules. (A) LDH concentration in cells in normoxic conditions; (B) ROS concentration in cells in normoxic conditions. (C) SOD concentration in cells in normoxic conditions. (D) LDH concentration in cells in hypoxic conditions. (E) ROS concentration in cells in hypoxic conditions. (F) SOD concentration in cells in hypoxic conditions. *P<0.05, **P<0.01, ****P<0.0001. NS, not significant; LDH, lactate dehydrogenase; ROS, reactive oxygen species; SOD, superoxide dismutase; NG1, normoxia and 0 mmol/l glucose group; NG2, normoxia and 0.5 mmol/l glucose group; NG3, normoxia and 3 mmol/l glucose group; NG4, normoxia and 5.5 mmol/l glucose group; NC, normoxia and control (22.5 mmol/l) group; HG1, hypoxia and 0 mmol/l glucose group; HG2, hypoxia and 0.5 mmol/l glucose group; HG3, hypoxia and 3 mmol/l glucose group; HG4, hypoxia and 5.5 mmol/l glucose group; HC, hypoxia and control (22.5 mmol/l) group.

AMPK activity is likely a direct result of the decline of mitochondrial function (34). In the present study, the glucose-free group exhibited decreased quantities of mitochondria, the mitochondrial morphology was swollen and deformed, and AMPKα1 expression was significantly downregulated. It was therefore demonstrated that AMPKα1 expression was directly associated with glucose concentration.

A proposed mechanism for the link between AMPK signaling and inflammation is shown in Fig. 7. AMPK is activated when cellular AMP/ATP levels change due to physiological stress or drug-induced effects. The AMPK signaling pathway mediates immune inflammation. High AMPK expression promotes the production of sirtuin 1, forkhead box protein O and peroxisome proliferator-activated receptor γ coactivator 1-α, thereby protecting cells from mitochondrial dysfunction, endoplasmic reticulum stress and oxidative stress, whilst inhibiting NF-κB signaling. NF-κB plays a key regulatory role in the immune inflammatory response. When the expression of AMPK is low, cells are no longer protected and NF-κB signaling is enhanced (35). Thus, the level of AMPK is closely related to the presence and function of mitochondria, and glucose concentration is key to maintaining the function of AMPK and may be the primary cause of cell aging.

The investigation into energy metabolism in the present study showed that glycolysis is the primary form of metabolism in TMJ disc cells, in an environment with sufficient glucose and

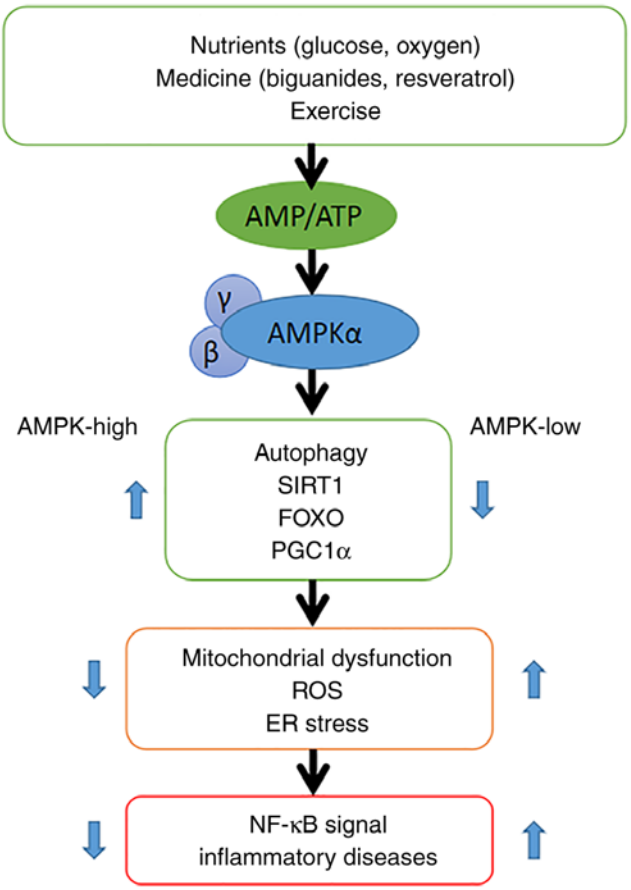

Figure 7. Relationship between the APMK signaling pathway and inflammation. AMPK, adenosine 5'-monophosphate-activated protein kinase; SIRT1, sirtuin 1; FOXO, forkhead box protein O; PGCα, peroxisome proliferator-activated receptor-γ coactivator α1; ROS, reactive oxygen species; ER, endoplasmic reticulum.

oxygen. Both metabolic mechanisms glycolysis and oxidative phosphorylation were inhibited when glucose and oxygen were insufficient, which means the Pasteur effect did not occur in sheep TMJ disc cells. The Pasteur effect means that glycolysis in biological cells and tissues will increase when oxygen is reduced. The Seahorse XFe test demonstrated that under normoxic conditions, the basal OCAR and glycolysis potential increased. Under hypoxic conditions, respiratory metabolism was inhibited, and the function of glycolysis and oxidative phosphorylation was significantly decreased. A previous study has confirmed that there is no Pasteur effect in chondrocytes but there is a Pasteur effect in TMJ articular disc cells (17). If the Pasteur effect existed in TMJ disc cells, the glycolysis rate would increase with the lack of oxygen supply, resulting in glucose depletion, more lactic acid, and low pH, leading to more extensive cell death (23). If the Pasteur effect did not exist in TMJ disc cells, the rate of glycolysis would be downregulated in hypoxia and the cells would maintain low glucose consumption, which would have a protective effect of the cells. The results of the present study demonstrated that the Pasteur effect did not occur in sheep TMJ disc cells. Thus, it was speculated that this is a self-protection mechanism for TMJ disc cells.

A study has found that the OCAR of degenerative intervertebral disc cells is three to five times higher than that of normal disc cells and that these degenerative cells may have been converted to a more oxidative phenotype (36). Meanwhile, chondrocytes can restore their phenotype under hypoxic conditions (37). Hypoxia has a major effect on the phenotypic maintenance of TMJ disc cells. In previous studies, sheep TMJ disc cells show reduced autophagy and apoptosis rates and increased cell survival under hypoxic conditions (21,22). This is beneficial for these dedifferentiated cells to achieve phenotypic reversal and produce more extracellular matrix. The results of the present study showed that the expression levels of Col-I and Col-II is downregulated during hypoxia. However, whether this helps to maintain the phenotype of articular disc cells requires further research.

From the results of the present study, it is demonstrated that glucose deficiency is a key factor in the degeneration of articular disc cells, and we suggest that regulating glucose concentration could be a viable treatment for tissue degeneration. Different drugs can regulate mitochondrial function and the respiratory metabolism of organisms through different mechanisms. It has been reported that AMPK can mediate the response to biguanide treatment, affect mitochondrial function and regulate blood glucose (38). Resveratrol can improve the ROS scavenging activity of SOD, thereby improving mitochondrial membrane potential and promoting mitochondrial biogenesis and function (39). However, to understand which drug could be effective in treating degenerative disease requires further research.

In conclusion, the present study demonstrated that the metabolism of TMJ disc cells is primarily glycolytic under physiological conditions. Hypoxic conditions and normal glucose concentrations may be suitable for the growth of TMJ disc cells. Glucose is a necessary nutrient to ensure cell survival, extracellular matrix synthesis, and mitochondrial function. Glucose deficiency may be related to disc degeneration, aging, and disease mechanisms. Future studies should focus on how glucose concentration can be adjusted under physiological conditions in TMJ cells in order to find a treatment for degeneration.

Acknowledgements

The authors would like to thank Dr Jing-ying Liu and Dr Hui Ren (School of Stomatology, Lanzhou University, Lanzhou, China) for their assistance in tissue sample preparation and Professor She-Ning Qi (Department of Histology and Embryology, School of Basic Medical Sciences, Lanzhou University, Lanzhou, China) for his linguistic assistance during the preparation of this manuscript. They also thank Professor Ben-Zhong Zhang (School of Public Health, Lanzhou University, Lanzhou, China) for his help with the statistical model and analysis.

Funding

The present study was supported by the Natural Science Foundation of Gansu Province (grant no. 21JR7RA161) and the Fundamental Research Funds for the Central Universities of NWMU (grant no. 31920220013).

Availability of data and materials

All data generated or analyzed during this study are included in this published article.

Authors' contributions

HK and GB conceived and designed the project. FD and PZ participated in cell culture and detection of cell proliferation, RT-PCR, Seahorse XF Glycolysis stress test, flow cytometry, fluorescence detection and ELISA. FD, GB and HK completed the draft preparation. FD and BM performed the statistical analysis. All authors took part in the discussion and revision of the manuscript before submission. All authors have read and approved the final manuscript. FD, HK and GB confirm the authenticity of all the raw data.

Ethics approval and consent to participate

All animal procedures were approved by The Animal Ethics Committee of the School of Stomatology, Northwest Minzu University (Lanzhou, China) and complied with its requirements (approval no. XBMZ YX-2021004).

Patient consent for publication

Not applicable.

Competing interests

The authors declare that they have no competing interests.

References

1. Gauer RL and Semidey MJ: Diagnosis and treatment of temporomandibular disorders. Am Fam Physician 91: 378-386, 2015.
2. Murphy MK, MacBarb RF, Wong ME and Athanasiou KA: Temporomandibular disorders: A review of etiology, clinical management, and tissue engineering strategies. Int J Oral Maxillofac Implants 28: e393-e414, 2013.
3. Liu F and Steinkeler A: Epidemiology, diagnosis, and treatment of temporomandibular disorders. Dent Clin North Am 57: 465-479, 2013.
4. Tanaka E, Detamore MS and Mercuri LG: Degenerative disorders of the temporomandibular joint: Etiology, diagnosis, and treatment. J Dent Res 87: 296-307, 2008.
5. Lu K, Ma F, Yi D, Yu H, Tong L and Chen D: Molecular signaling in temporomandibular joint osteoarthritis. J Orthop Translat 32: 21-27, 2021.
6. Cha S, Lee SM, Wang J, Zhao Q and Bai D: Enhanced circadian clock in MSCs-based cytotherapy ameliorates age-related temporomandibular joint condyle degeneration. Int J Mol Sci 22: 10632, 2021.
7. Nascimento GC, De Paula BB, Gerlach RF and Leite-Panissi CRA: Temporomandibular inflammation regulates the matrix metalloproteinases MMP-2 and MMP-9 in limbic structures. J Cell Physiol 236: 6571-6580, 2021.
8. Sagl B, Schmid-Schwap M, Piehslinger E, Rausch-Fan X and Stavness I: An in silico investigation of the effect of bolus properties on TMJ loading during mastication. J Mech Behav Biomed Mater 124: 104836, 2021.
9. Chapman J, Fielder E and Passos JF: Mitochondrial dysfunction and cell senescence: Deciphering a complex relationship. FEBS Lett 593: 1566-1579, 2019.
10. Wu Y, Cisewski SE, Coombs MC, Brown MH, Wei F, She X, Kern MJ, Gonzalez YM, Gallo LM, Colombo V, *et al*: Effect of sustained joint loading on TMJ disc nutrient environment. J Dent Res 98: 888-895, 2019.
11. Messina OD, Wilman MV and Neira LF: Nutrition, osteoarthritis and cartilage metabolism. Ageing Clin Exp Res 31: 807-813, 2019.
12. Mamun AA, Hayashi H, Yamamura A, Nayeem MJ and Sato M: Hypoxia induces the translocation of glucose transporter 1 to the plasma membrane in vascular endothelial cells. J Physiol Sci 70: 44, 2020.
13. Richardson SM, Hoyland JA, Mobasheri R, Csaki C, Shakibaei M and Mobasheri A: Mesenchymal stem cells in regenerative medicine: Opportunities and challenges for articular cartilage and intervertebral disc tissue engineering. J Cell Physiol 222: 23-32, 2010.
14. Kulkarni AC, Kuppusamy P and Parinandi N: Oxygen, the lead actor in the pathophysiologic drama: Enactment of the trinity of normoxia, hypoxia, and hyperoxia in disease and therapy. Antioxid Redox Signal 9: 1717-1730, 2007.
15. Adesida AB, Mulet-Sierra A and Jomha NM: Hypoxia mediated isolation and expansion enhances the chondrogenic capacity of bone marrow mesenchymal stromal cells. Stem Cell Res Ther 3: 9, 2012.
16. Holm S, Maroudas A, Urban JP, Selstam G and Nachemson A: Nutrition of the intervertebral disc: Solute transport and metabolism. Connect Tissue Res 8: 101-119, 1981.
17. Lee RB and Urban JP: Evidence for a negative Pasteur effect in articular cartilage. Biochem J 321: 95-102, 1997.
18. Kuo J, Shi C, Cisewski S, Zhang L, Kern MJ and Yao H: Regional cell density distribution and oxygen consumption rates in porcine TMJ discs: An explant study. Osteoarthritis Cartilage 19: 911-918, 2011.
19. Wright GJ, Kuo J, Shi C, Bacro TR, Slate EH and Yao H: Effect of mechanical strain on solute diffusion in human TMJ discs: An electrical conductivity study. Ann Biomed Eng 41: 2349-2357, 2013.
20. Shi C, Kuo J, Bell PD and Yao H: Anisotropic solute diffusion tensor in porcine TMJ discs measured by FRAP with spatial Fourier analysis. Ann Biomed Eng 38: 3398-3408, 2010.
21. Xiaolan H, Guangjie B, Linglu S, Xue Z, Shanying B and Hong K: Effect of different oxygen tension on the cytoskeleton remodeling of sheep temporomandibular joint disc cells. Hua Xi Kou Qiang Yi Xue Za Zhi 35: 362-367, 2017 (In Chinese).
22. Zhang F, Bao G and Tang Y: Effects of hypoxia on the apoptosis and autophagy of the goat temporomandibular joint disc cells after serum deprivation. Chin J Cell Biol 40: 1295-1302, 2018.
23. Cisewski SE, Zhang L, Kuo J, Wright GJ, Wu Y, Kern MJ and Yao H: The effects of oxygen level and glucose concentration on the metabolism of porcine TMJ disc cells. Osteoarthritis Cartilage 23: 1790-1796, 2015.
24. Mobasheri A, Bondy CA, Moley K, Mendes AF, Rosa SC, Richardson SM, Hoyland JA, Barrett-Jolley R and Shakibaei M: Facilitative glucose transporters in articular chondrocytes. Expression, distribution and functional regulation of GLUT isoforms by hypoxia, hypoxia mimetics, growth factors and pro-inflammatory cytokines. Adv Anat Embryol Cell Biol 200: 1-84, 2008.
25. Carling D, Mayer FV, Sanders MJ and Gamblin SJ: AMP-activated protein kinase: Nature's energy sensor. Nat Chem Biol 7: 512-518, 2011.
26. Zheng L, Zhang Z, Sheng P and Mobasheri A: The role of metabolism in chondrocyte dysfunction and the progression of osteoarthritis. Ageing Res Rev 66: 101249, 2021.
27. Bibby SR and Urban JP: Effect of nutrient deprivation on the viability of intervertebral disc cells. Eur Spine J 13: 695-701, 2004.
28. Amorim JA, Coppotelli G, Rolo AP, Palmeira CM, Ross JM and Sinclair DA: Mitochondrial and metabolic dysfunction in ageing and age-related diseases. Nat Rev Endocrinol 18: 243-258, 2022.
29. Ramasamy TS, Yee YM and Khan IM: Chondrocyte aging: The molecular determinants and therapeutic opportunities. Front Cell Dev Biol 9: 625497, 2021.
30. Gogvadze V and Orrenius S: Mitochondrial regulation of apoptotic cell death. Chem Biol Interact 163: 4-14, 2006.
31. Henrotin Y, Kurz B and Aigner T: Oxygen and reactive oxygen species in cartilage degradation: Friends or foes? Osteoarthritis Cartilage 13: 643-654, 2005.
32. Petursson F, Husa M, June R, Lotz M, Terkeltaub R and Liu-Bryan R: Linked decreases in liver kinase B1 and AMP-activated protein kinase activity modulate matrix catabolic responses to biomechanical injury in chondrocytes. Arthritis Res Ther 15: R77, 2013.
33. Terkeltaub R, Yang B, Lotz M and Liu-Bryan R: Chondrocyte AMP-activated protein kinase activity suppresses matrix degradation responses to proinflammatory cytokines interleukin-1β and tumor necrosis factor α. Arthritis Rheum 63: 1928-1937, 2011.

34. Wang Y, Zhao X, Lotz M, Terkeltaub R and Liu-Bryan R: Mitochondrial biogenesis is impaired in osteoarthritis chondrocytes but reversible via peroxisome proliferator-activated receptor γ coactivator 1α. Arthritis Rheumatol 67: 2141-2153, 2015.
35. Andris F and Leo O: AMPK in lymphocyte metabolism and function. Int Rev Immunol 34: 67-81, 2015.
36. Cisewski SE, Wu Y, Damon BJ, Sachs BL, Kern MJ and Yao H: Comparison of oxygen consumption rates of nondegenerate and degenerate human intervertebral disc cells. Spine (Phila Pa 1976) 43: E60-E67, 2018.
37. Adesida AB, Mulet-Sierra A, Laouar L and Jomha NM: Oxygen tension is a determinant of the matrix-forming phenotype of cultured human meniscal fibrochondrocytes. PLoS One 7: e39339, 2012.
38. Di Magno L, Di Pastena F, Bordone R, Coni S and Canettieri G: The mechanism of action of biguanides: New answers to a complex question. Cancers (Basel) 14: 3220, 2022.
39. Zhou J, Yang Z, Shen R, Zhong W, Zheng H, Chen Z, Tang J and Zhu J: Resveratrol improves mitochondrial biogenesis function and activates PGC-1α pathway in a preclinical model of early brain injury following subarachnoid hemorrhage. Front Mol Biosci 8: 620683, 2021.